

# Accurate study on the surface of an oblique incidence total internal reflection quarter phase retarders and how it affects their performance

N. A. Mahmoud

*Length and Engineering precision, National Institute for Standards (NIS), Tersa st., P. O. B 136, Giza 12211, Egypt.*

✉ E-mail: [naglaamahmoud2006@yahoo.com](mailto:naglaamahmoud2006@yahoo.com)

Received: 26/12/2021

Accepted: 02/08/2022

DOI: 10.7149/OPA.55.3.55100

## Abstract:

The performance of many optical glass elements depends on the structure of the surface. The high refractive index of flint glass is advantageous in constructing some optical elements (lenses, prisms, beam splitters, ...). Also, high achromaticity and size reduction in oblique incidence TIR (total internal reflection) phase retarders require high-index glass. The present work is interested in studying the use of ellipsometry as a precise and accurate technique to test changes in optical properties of the thin layer formed on an oblique incidence TIR quarter phase retarder at different wavelengths which affects some optical properties such as the retardance value of the rhomb retarder, to adjust and make the needed corrections.

## Keywords:

Optical glass, ellipsometry, oblique incidence retarder, surface layer, and retardance.

## REFERENCES AND LINKS / REFERENCIAS Y ENLACES

- [1] M. Mazza, B. Farnoux, F. Samuel. C. Sella and P. Trocellier. Effect of mechanical polishing on surface structure of glasses studied by grazing angle neutron reflectometry. *Optics Communications*, **100**, 220 – 30 (1993)
- [2] A. Ledieu, F. Devreux and P. Barboux. Monte Carlo simulation of borosilicate glass corrosion: predictions for morphology and kinetics. *J. Non Cryst. Solids* **345, 346**, 715 – 19 (2004)
- [3] E. C. Ziemath, Degradation of the surface of a metasilicate glass due to atmosphere moisture. *Quim. Nova* **21** (3), 365 – 60 (1998)
- [4] F. Fujiwara, J. Koh, P. I. Rovira and R. W. Collins Assessment of effective medium theories in the analysis of nucleation and microscopic surface roughness evolution for semiconductor thin films. *Phys. Rev. B*, **61** (16), 10832 – 44(2000)
- [5] Çolak, O., C. Kubanoğlu and M/ Cengiz Kayacan, Milling surface roughness prediction using evolutionary programming methods. *Matter. Design*, **28**, 657 (2007)
- [6] Dennis Goldstein in: 'polarized light', Second Edition, Marcell Dekker, Inc. (2003)
- [7] N. A. Mahmoud. Studies on some optical polarization elements and measurements. M. Sc. Thesis, Faculty of Science, Cairo University (2007)
- [8] N. N. Nagib and S. A. Khodier. Optimization of a rhomb-type quarter-wave phase retarder. *Appl. Opt.* **34**, 2927 – 30 (1995)
- [9] N. N. Nagib. Theory of oblique phase retarders. *Appl. Opt.* **36**, 1547 – 52 (1997)



- [10] R. J. King, Quarter-wave retardation system based on the Fresnel rhomb principle, *J. Sci. Instrum.* **43**, 617-622 (1996)
- [11] J. M. Bennett and R. J. King. Effect of polishing technique on the roughness and residual film on fused quartz optical flats. *Appl. Opt.* **9** (1), 236 – 238 (1970)
- [12] N. N. Nagib, N. A. Mahmoud, M. S. Barhawi. Realization and calibration of an oblique incidence rhomb retarder of extreme retardance stability. *Measurement.* **124**, 156-158 (2018)
- [13] N. N. Nagib. Four-measurement technique for elimination of errors in phase plates calibration. *Meas. Sci. Technol.* **15**, 1166 – 74 (2004)

## 1. Introduction

The optical glass used in manufacturing optical elements or devices is subjected to mechanical polishing, chemical etching, or other processes to improve the quality of its surfaces. The performance of many optical glass elements depends on the structure of the surface. Thus, a clean and smooth surface with a similar composition to that of the bulk glass is essentially required in many optical elements. But unfortunately, the previous requirements cannot be easily achieved due to different factors which are essential in the surface layer formation, such as surface treatment, glass degradation, and environmental effects. In most cases, the formed surface layers are studied using a single homogeneous surface film model and an effective medium model that describes the surface's nano roughness [1-4].

Quality control of the functional surface of optical glasses is one of the most important factors and must be precise to give an optimal functional state, the required speed, and an economical state. There are many methods for measuring the surface roughness of glasses, such as image processing, microscopes, stylus-type instruments, profile tracing instruments, etc., [5]. The contact methods for the determination of roughness are undesirable because they are destructive and leave prints on the tested surface. The ellipsometric technique can be used to determine the optical constants and the surface thickness and roughness of the bulk optical glass. It has several advantages over other methods. Among these are the simplicity of measurement and the ease of sample preparation. Besides, it is non-destructive and requires only a very small sample size.

Ellipsometry can be conveniently divided into two parts, the first is the measurement technique for determining  $\psi$  and  $\Delta$ , which describe the change in amplitude and phase in the reflected wave. The second is the theory required to relate the optical parameters of the thin film formed on the substrate, (the refractive index  $n$ , the extinction coefficient  $k$ , and the thickness  $d$ ) to the measured values of  $\psi$  and  $\Delta$ .

Fig. 1 represents a thin film of thickness  $d$  and optical constants  $n_1, k_1$  over the substrate.  $E_p$  and  $E_s$  are the components of the incident field in the plane of incidence and perpendicular to the plane of incidence. The components of the reflected field are  $R_p$  and  $R_s$ .

For the incident and the reflected fields, suppressing the propagation factor,

$$E_p = E_{0p} e^{i\alpha_p}, \quad (1a)$$

$$E_s = E_{0s} e^{i\alpha_s}, \quad (1b)$$

$$R_p = R_{0p} e^{i\beta_p}, \quad (2a)$$

$$R_s = R_{0s} e^{i\beta_s}. \quad (2b)$$

Where  $(\alpha_p, \alpha_s)$  and  $(\beta_p, \beta_s)$  are the phases of the incident and reflected components.

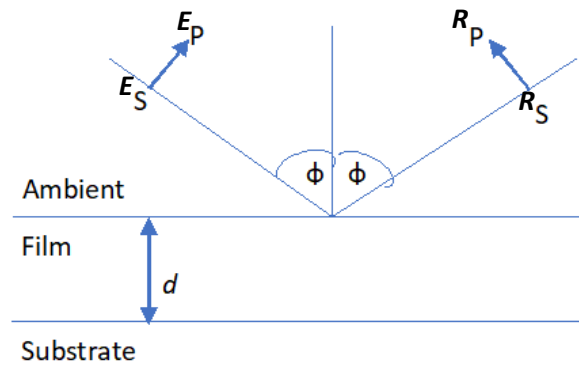


Figure 1: Film/substrate structure.  $d$  is the film thickness,  $p$  and  $s$  are the parallel and perpendicular components of the incident and reflected light, and  $\phi$  is the angle of incidence.

Introducing the complex reflection coefficients  $\rho_p, \rho_s$  relating the reflected field components to the incident field components.

$$R_p = \rho_p E_p, \quad (3a)$$

$$R_s = \rho_s E_s. \quad (3b)$$

Defining a complex relative amplitude attenuation  $\rho$  as

$$\rho = \rho_p / \rho_s. \quad (4)$$

Then,

$$\rho = [(R_{0p}/E_{0p}) / (E_{0s}/R_{0s})] e^{i(\beta-\alpha)} \quad (5)$$

where  $\alpha = \alpha_p - \alpha_s$  and  $\beta = \beta_p - \beta_s$ .

We can express  $\Delta = (\beta - \alpha)$  and  $\tan \psi = (R_{0p}/E_{0p}) / (E_{0s}/R_{0s})$ , so

$$\rho = \tan \psi e^{i\Delta} = f(n, k \text{ and } d). \quad (6)$$

Since, we study the surface of glass retarder which is transparent in the visible spectrum ( $k = 0$ ),

$$\rho = \tan \psi e^{i\Delta} = f(n, d), \quad (7)$$

which is called the fundamental equation of ellipsometry. At a given angle of incidence  $\phi$  and the value of  $n_g$  (the refractive index of the glass) which is known in advance, and the values of  $\psi$  and  $\Delta$  found by using ellipsometric analysis, the main issue here is to relate the previous mentioned values to  $n$  and  $d$  [6].

The present work was initiated by the fact that, on calibrating an oblique-incidence TIR  $4/\lambda$  phase retarder [7], Fig. 2 at wavelength 589 nm, it was found that the device provided a retardance of  $87.00^\circ$  with uncertainty  $\pm 0.12^\circ$ , *i. e.*,  $3^\circ$  less than the theoretically calculated value, as the rhomb was calibrated by using the "Four-measurement technique for elimination of errors in phase plate calibration" [13].

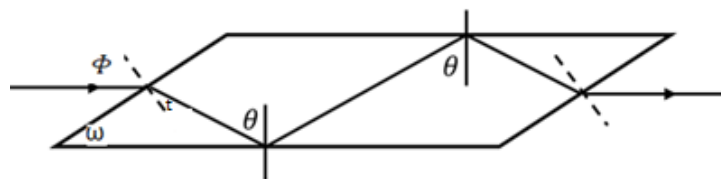


Figure 2: Oblique incidence TIR  $\lambda/4$  phase retarder,  $n_g = 1.70002$  at 589 nm.

This difference could be attributed to several factors, including errors in the external angle of incidence, birefringence in the bulk glass, a manufacturing error in the acute angle or the formation of surface layers on the reflecting surfaces. This device belongs to a class of total internal reflection (TIR) phase retarders known as oblique-incidence retarders. In this class, the angle of (TIR) is not of fixed value but varies with the refractive index  $n$  of the used glass (or equivalently, with the wavelength  $\lambda$  of the incident light) [8, 9], such that

$$\theta = \omega + t \quad (8)$$

and

$$t = \sin^{-1} (\sin \Phi / n), \quad (9)$$

where  $\omega$  is the angle between the entrance face and the reflecting surface,  $\Phi$  is the angle of incidence, and  $t$  is the angle of refraction. The previous equation shows that, for the same incidence value, the angle of  $t$  varies with  $n$  (or with  $\lambda$ ). Thus,  $\theta$  is no longer of a fixed value, and the retardance is expressed as:

$$\delta = f(n, \theta), \quad (10)$$

$$\text{where } \theta = f_1(n) \text{ and } n = f_2(\lambda). \quad (11)$$

The present work is interested in studying the optical properties of the thin surface layer formed on this TIR rhomb retarder which is made of flint glass ( $n_g = 1.70002$  at 589 nm) at spectral wavelengths from 400 – 800 nm in steps of 100 nm, and will study the effect of this formed layer on the performance of this TIR rhomb retarder. The effective medium approximation can then be used to analyze the measured ellipsometric values, assuming the effective medium layer consists of a physical mixture interface of air and glass. An ellipsometric technique is used to determine the amplitude and phase of the reflected beam, and then an effective medium approximation is used to obtain the refractive index and thickness.

## 2. Experimental work

We studied the surface layer formed on one of the two reflecting faces of the TIR rhomb retarder shown in Fig. 2, which is made of flint glass ( $n_g = 1.70002$  at 589 nm). The measuring equipment used is a Spectroscopic ellipsometer PHE103 (Angstrom Advanced Inc.). It is an automated version supported by analyzing software. The sample is placed on a motorized stage controlled by the software and enables fine adjustment of the incidence angle, and the ellipsometric angles are measured with an accuracy of  $\pm 0.01^\circ$ . A schematic diagram of the ellipsometer is presented in Fig. 3, which consists of a light source, polarizer, analyzer, a quarter-phase plate (compensator),  $\Phi$  is the angle of incidence, and detecting system. The angle of incidence  $\Phi$  was set at ( $\Phi = 60^\circ, 65^\circ, 70^\circ$ ). At a temperature of  $(20 \pm 0.05)^\circ\text{C}$ , measurements were carried out in the spectral wavelengths of 400 – 800 nm in 100 nm steps.

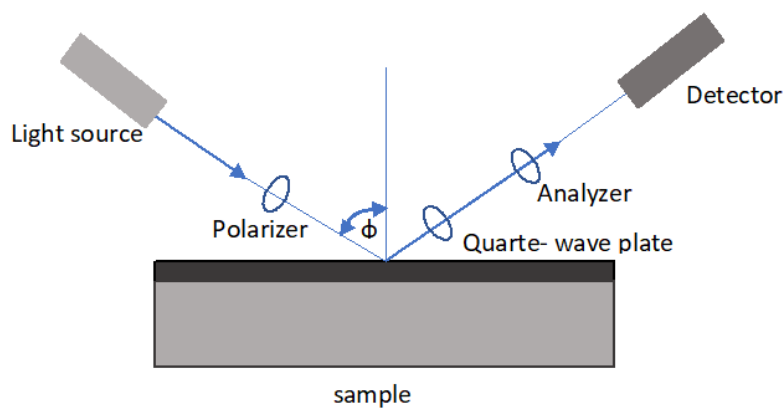


Figure 3: Ellipsometric schematic diagram.

### 3. Results

The values of the ellipsometric parameters  $\psi$  and  $\Delta$  according to the angles of incidence within the interval  $60^\circ$  and  $70^\circ$  are gathered in table 1 and Figs. 4 and 5.

Table 1: Values of  $\psi$  and  $\Delta$  versus the wavelengths for different values of angle of incidence.

| Wavelength,<br>$\lambda$ nm | $\phi=60^\circ$        |                          | $\phi=65^\circ$        |                          | $\phi=70^\circ$        |                          |
|-----------------------------|------------------------|--------------------------|------------------------|--------------------------|------------------------|--------------------------|
|                             | $\Psi$<br>( $^\circ$ ) | $\Delta$<br>( $^\circ$ ) | $\Psi$<br>( $^\circ$ ) | $\Delta$<br>( $^\circ$ ) | $\Psi$<br>( $^\circ$ ) | $\Delta$<br>( $^\circ$ ) |
| 400                         | 7.69                   | 13.57                    | 14.79                  | 7.26                     | 22.28                  | 3.9                      |
| 500                         | 7.13                   | 15.74                    | 14.30                  | 7.96                     | 21.77                  | 4.59                     |
| 600                         | 6.73                   | 15.79                    | 13.98                  | 8.02                     | 21.41                  | 4.83                     |
| 700                         | 6.44                   | 15.14                    | 13.77                  | 7.45                     | 21.17                  | 4.27                     |
| 800                         | 6.25                   | 14.27                    | 13.63                  | 7.00                     | 21.00                  | 3.97                     |

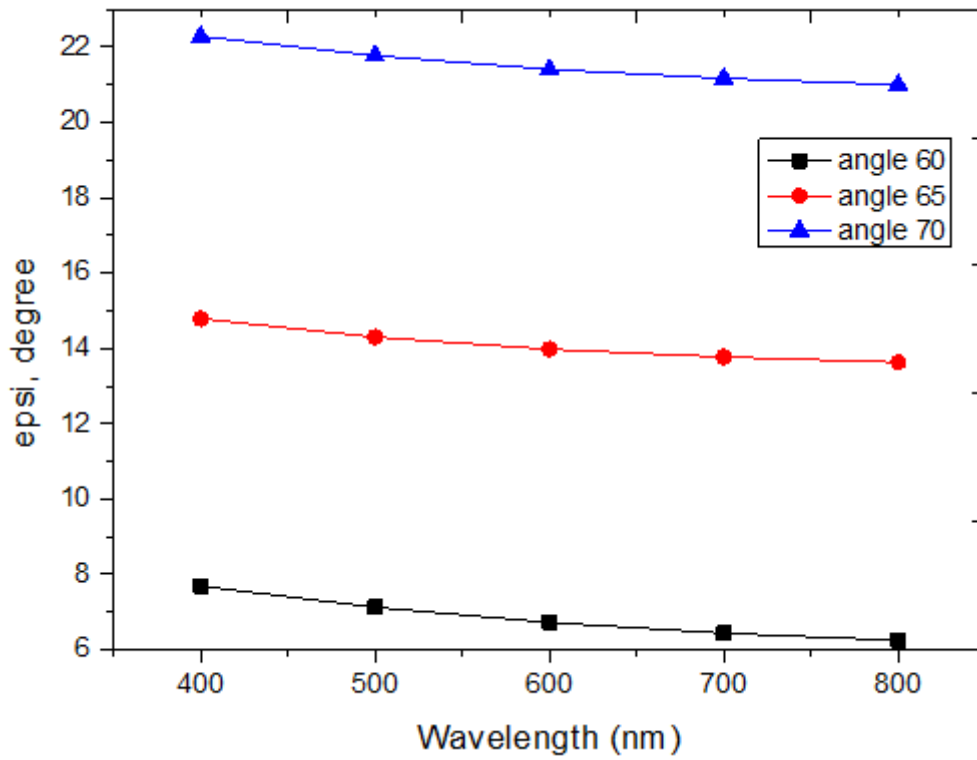


Figure 4: The variation of  $\Psi$  versus the wavelength for different angles of incidence.

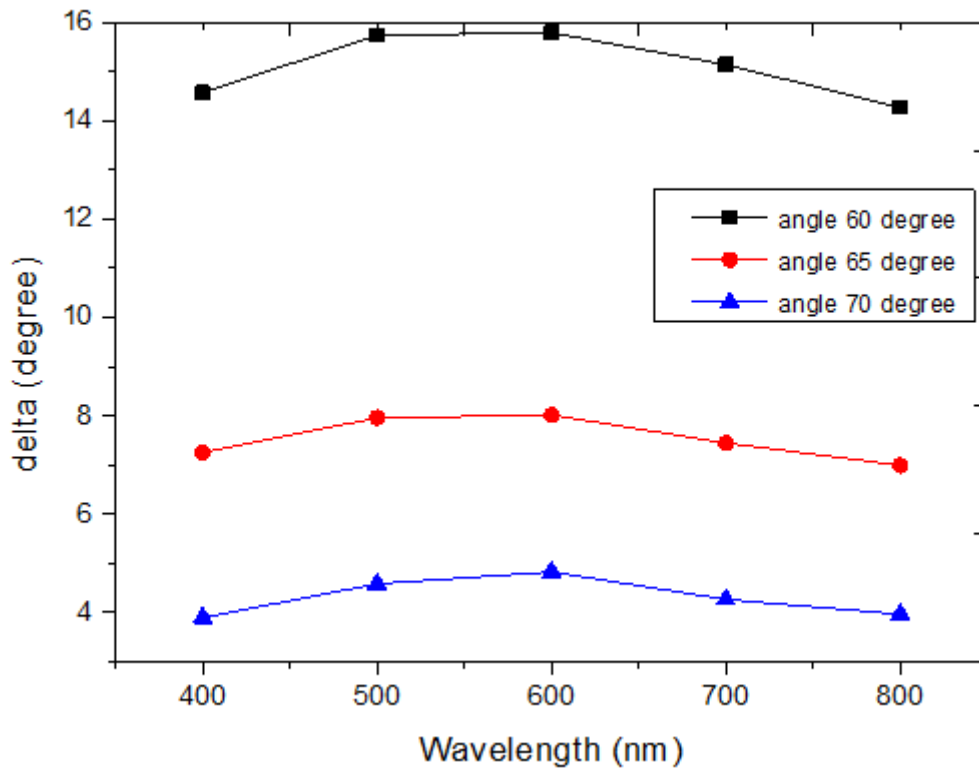


Figure 5: The variation of  $\Delta$  versus the wavelength for different angles of incidence.

The values obtained from table 1 allow drawing up table 2 and figure 6 as a result of the analysis software of the spectroscopic ellipsometer PHE103 (Angstrom Advanced Inc.), with an uncertainty of 0.0164 for the values of  $n_f$ , (the refractive index of the layer formed on the surface of the glass) versus the spectral wavelengths, from (400–800) nm in steps of 100 nm for different angles of incidence.

Table 2: Values of the refractive index versus the wavelengths for different angles of incidence.

| Wavelength,<br>$\lambda$ nm | $n_f$<br>( $\Phi = 60^\circ$ ) | $n_{fz}$<br>( $\Phi = 65^\circ$ ) | $n_f$<br>( $\Phi = 70^\circ$ ) |
|-----------------------------|--------------------------------|-----------------------------------|--------------------------------|
| 400                         | 1.6440                         | 1.6566                            | 1.6466                         |
| 500                         | 1.6125                         | 1.6289                            | 1.6489                         |
| 600                         | 1.5975                         | 1.6134                            | 1.5934                         |
| 700                         | 1.5890                         | 1.5915                            | 1.5899                         |
| 800                         | 1.5834                         | 1.5945                            | 1.5802                         |

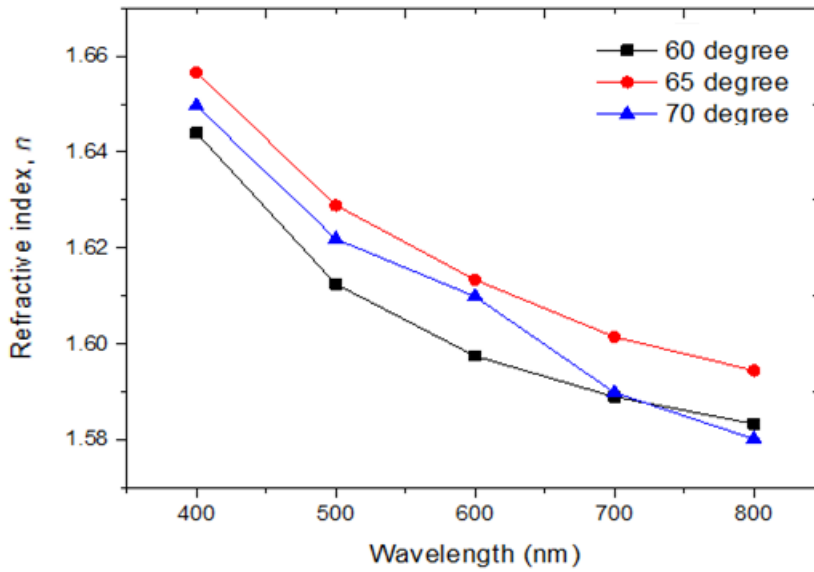


Figure 6: The variation of  $n_f$  versus the wavelength for different angles of incidence..

Also, the values of the thickness of the formed layer  $d_f$  according to the angles of incidence within the interval  $60^\circ$  and  $70^\circ$  are shown in Table 3 with an uncertainty of  $\pm 0.04\text{nm}$ .

Table 3: Values of the thickness of the formed layer versus the angle of incidence.

| Angle of incidence, $\phi(^{\circ})$ | $d_f$ (nm) |
|--------------------------------------|------------|
| 60                                   | 121.05     |
| 65                                   | 120.23     |
| 70                                   | 125.12     |

Table 4 and Figure 7 show the differences between the average refractive index for the formed layer  $n_f$  and that of the glass substrate  $n_s$ .

Table 4: The refractive index of the formed layer and that of the glass versus the wavelength.

| Wavelength, $\lambda$ nm | $n_f$ (average) | $n_s$  |
|--------------------------|-----------------|--------|
| 400                      | 1.6491          | 1.7440 |
| 500                      | 1.6301          | 1.7125 |
| 600                      | 1.6014          | 1.6975 |
| 700                      | 1.5901          | 1.6890 |
| 800                      | 1.5860          | 1.6834 |

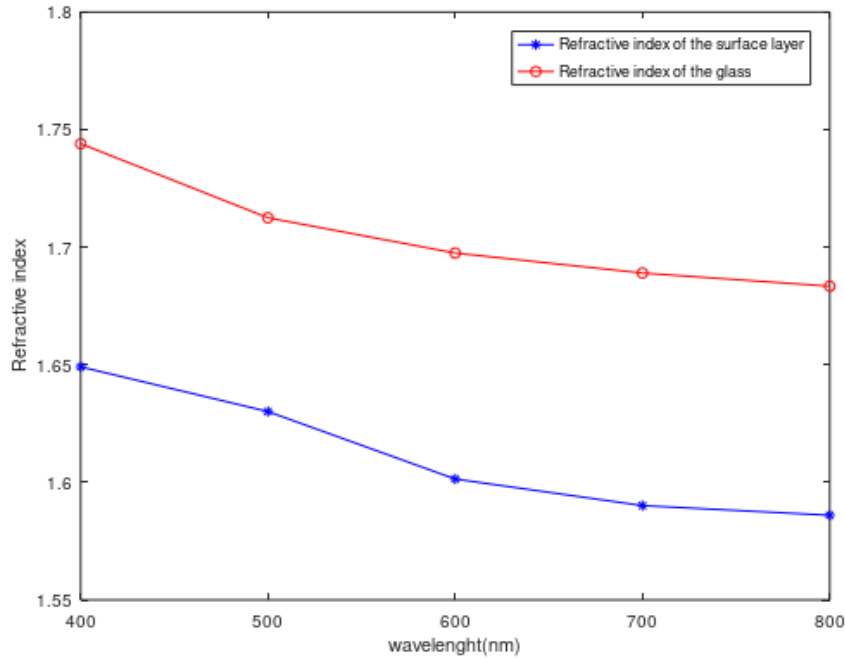


Figure 7 : The differences between the refractive index for the formed layer  $n_f$  and that of the glass substrate  $n_s$ .

From the analytical study of the glass surface using the ellipsometric method, the average  $n_f$  for  $60^\circ$ ,  $65^\circ$  and  $70^\circ$  angles of incidence, at 589 nm wavelength, equals 1.6000, and, extracted from table 3,  $d_f$  equals 122.13 nm.

#### 4. Discussion

The experimental results showed a reduction of approximately 0.10 compared to the refractive index of the glass of the rhomb for all wavelengths. The main factor for this reduction is the formation of a surface layer on the sides of the rhomb, which in turn explains the large reduction in the retardance value of the rhomb ( $-3^\circ$ ) during the calibration of the rhomb retarder. Other factors are the polishing effects and internal stresses [10]. In many optical measurements, the surface layer, usually present on most glasses, is neglected either because it does not affect the measurement or because its effect is negligible. However, for measurements made using polarized light, particularly in ellipsometric measurements, the homogeneity of the studied surface is extremely important [11].

According to the relation,

$$\theta = \omega + t = \alpha + \sin^{-1}(\sin \Phi / n), \quad (12)$$

where  $\Phi$  and  $t$  are the angles of incidence and refraction on the entrance face, we notice that the angle  $t$  varies with  $n$ . Thus,  $\theta$  is no longer of a fixed value, and, in this case, the retardance is expressed as in equations (10) and (11).

The retardance of our rhomb could be adjusted to a value close to  $90^\circ$  by a small variation in the external angle of incidence  $\Phi$  [12]. We note that variations in the external angle of incidence  $\Phi$  could be compensated for the variation of  $n$ . Thus, the device retardance can be adjusted at will by simply changing the angle  $\Phi$ .

#### 5. Conclusion

This work describes the use of ellipsometry as a precise and accurate technique to test and monitor changes in surfaces of optical components because of manufacturing or environmental surroundings, which affect some optical measurements, such as the retardance value of TIR rhomb retarder, to adjust and make corrections in the result values.

